Alexandria Journal of Soil and Water Sciences (AJSWS) Volume: 9 (1)

Using Satellite Imagery to Analyze Land Use and Land Cover Changes (LULC) in the Motobus Area Ecosystem, Nile Delta, Egypt

Azza E. A. Elsharkawy[1], I. Morsy[2], G. Abdel-Nasser[1], Wafaa H. M. Aly[1], Hoda A. Mahmoud[1]

[1] **Soil and Agricultural Chemistry Department, Faculty of Agriculture (Saba Basha), Alexandria University,**

[2] **Soil, Water and Environment Res. Inst. (SWERI), Agricultural Research Center (ARC), Giza, Egypt.**

DOI: 10.21608/ajsws.2025.331467.1021

Article Information

Received: October 1st 2024

Revised: November 11, 2024

Accepted: December 31, 2024

Published: January 1st 2025

ABSTRACT : Understanding the changing dynamics of land use and land cover (LULC) is critical for efficient ecological management modification and sustainable land-use planning. This work aimed to identify and categorize seven Landsat satellite images over 50 years in Egypt's Nile Delta Motobus Area Ecosystem. In the present study, the detection of historical LULC change dynamics for a time from 1972 to 2022 was performed. We used seven Landsat images, acquired by different sensors, as spatial and temporal data sources for the study region. Moreover, the process of image categorization employed a supervised classification method. The results of the LULC change estimation between 1972 and 2022 revealed that the proportion of built-up areas in the study area increased from 5.5% in 1984 to 12.5% in 2022. This urban expansion came at the expense of converting previous agricultural lands into established cities and villages, as well as constructing new residential areas on undeveloped land. In addition, the proportion of cultivated land has risen from 56.45% of the total area in 1984 to 63.55% in 2022, primarily because of continuous soil reclamation initiatives in desert regions beyond the Nile Valley. Furthermore, from 1972 to 2022, desert regions saw a significant reduction in their total land area, losing around 50% of their original extent, whereas water bodies saw a minimal and negligible expansion. These trends are characterized by a decline in desert regions and an increase in recently restored urban and agricultural areas. Regarding the CA-Markov model validation, the Kappa indices varied between 0.86 and 0.93 for both the actual and simulated maps. This indicates that the model performed exceptionally well in predicting future trends in LULC. Therefore, using the CA-Markov hybrid model to predict and model future LULC trends is a promising way to monitor and mitigate the negative effects of LULC changes. This approach also aids land use policymakers and facilitates land management.

Keywords: *Spatio-temporal LULC, RS, GIS, Burullus Lake, MLC, LULC, soil unit map*

INTRODUCTION

Land degradation is a worldwide problem that arises from factors such as population growth, improper land use, forest loss, global warming, and other variables **(Bakr and Afifi, 2019)**. Understanding land use and land cover (LULC) changes in a region is critical for sustainable land management and development **(Das and Sarkar, 2019)** LULC change is accelerating in many developing nations due to rapid global economic and population growth, as well as globalization **(Iizuka et al., 2017)**. Various elements such as scale, time, politics, economy, and social factors influence LULC changes **(Calicioglu et al., 2019)**. LULC alterations have been identified as important factors in causing environmental changes at all geographical and temporal dimensions **(Adepoju et al., 2006)**. The changes above, including climate change, biodiversity loss, and pollution of water, soil, and air, are regarded as the utmost concerns for humanity **(Zabihi et al., 2020)**. LULC refers to the specific physical characteristics of the land, including forests, wetlands, impervious surfaces, agriculture, and water bodies **(Nath et al., 2020)**. It also encompasses how humans utilize these land types within a given area. Moreover, LULCs are geographically scattered as a result of the dynamic interplay between human activities and natural elements of ecosystems **(Nath et al., 2020; Zabihi et al., 2020)**. Various factors, including natural, social, and economic elements influence the intricate dynamics of LULC systems. The availability and distribution of LULC have a significant impact on climate, environmental issues, and the conditions of natural ecosystems **(Cihlar, 2000; Yan et al,. 2015)**. Moreover, alterations in global LULC are a primary source of considerable apprehension regarding future LULC patterns **(Srivastava et al., 2012)**. Furthermore, changes in LULC have a crucial role in the sustainability and management of natural resources **(Hou et al., 2019; Lombardi et al., 2020).** Scholars widely recognize satellite imagery as a valuable source of information for LULC analysis **(Saadat et al., 2011; Yuan et al., 2005)**. Although attempts to use different interpretation techniques for LULC mapping have been made since the mid-1970s satellite-based imaging remains the preferred method (Dewan and Yamaguchi 2009; Gomes et al. 2020). In recent decades, the field of science and technology has made significant progress, leading to the development and implementation of various LULC techniques worldwide **(Phiri and Morgenroth, 2017; Reimann et al., 2018).** Remote sensing (RS) and geographic information systems (GIS) techniques offer valuable methods for comprehending, examining, and tracking LULC changes in landscapes over time **(Armin et al., 2020; Kotaridis and Lazaridou, 2018)**. Several studies have utilized these techniques to investigate LULCs **(Hua, 2017; Liping et al., 2018; Rawat and Kumar, 2015).** When applied to a specific region, the periodic imaging data from Landsat provides a reliable data source for predicting patterns in land use and land cover (Jawak et al. 2015). Moreover, a range of methods have been developed to ascertain past and future LULC patterns. These models provide suitable methods for identifying the spatial

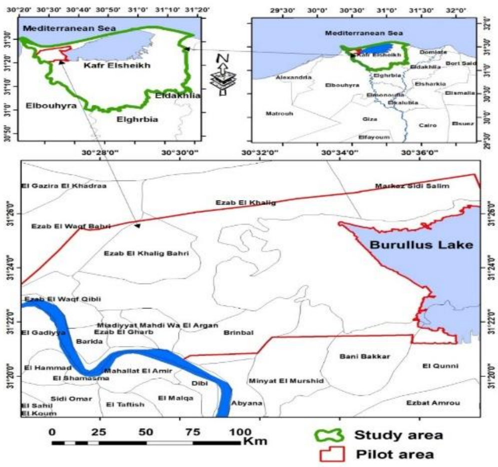

variability patterns in LULC. In addition, to get a good idea of how well the model predicts LULC changes in a certain area, it needs to be checked by comparing the expected changes in LULC with the actual changes (**Nath et al., 2020)**.The Nile Delta of Egypt is the third most vulnerable mega-delta to climate change, according to the IPCC **(Field et al., 2014).** Low-lying lands are often below sea level (BSL), so sea level rise (SLR) and climate change gradually flood them **(Chi and Ho, 2018; Derdouri et al., 2021; El-Shihy and Ezquiaga, 2019).** Inundation, degradation ,seawater infiltration, groundwater pollution, and estuarine and coastal water contamination are also common in coastal areas **(Masria et al., 2014; Nofal et al., 2015).** Due to these issues, it is essential to monitor historical land surface elevation variations to assess soil surface increases and decreases and determine specific surface elevation changes over time and space. Egypt has about five Mediterranean coastline lakes, from east to west, including Bardawil, Manzala, Burullus, Idku, and Mariout. Every lake in the northern Sinai Peninsula, except Lake Bardawil, is deltaic, revealing that Egypt's lakes, despite their economic importance, are contaminated, deteriorating, and under human and environmental stress **(Abd El-Hamid et al., 2021; Arowolo and Deng, 2018; El Kafrawy et al., 2019).** Desertification, infilling, and cultivation have reduced deltaic lake coverage. Deltaic lakes store industrial, agricultural, and domestic wastewater. These lakes were heavily polluted. Increasing sea levels affect northern shore lakes with saltwater intrusion. Lake size and neighboring land usage must be monitored **(Abd El-Hamid et al., 2021; Halim et al., 2013; Radwan, 2019).** This study emphasizes the combined use of remote sensing and GIS tools to detect changes in LULC in the Motobus region of Kafr El-Sheikh, Egypt. The study aims to accomplish three primary objectives. 1) Determine the LULC classes and classify them using satellite images and classification methods, 2) To create LULC maps for analyzing changes that took place from 1972 to 2022, and 3) To assess the precision of the LULC categories to understand the mapping error matrix. The study's findings can offer valuable insights into land-use development policies in the region.**Figure (1).** *General location of the study area*

Table (1). The monthly averages of the primary climatic parameters of the study area from 1981 to 2021

Parameters	Jan	Feb	March	April	May	June	July	August	Sept	Oct.	Nov.	Dec.
Minimum Temperature, C°	10.18	10.22	11.36	13.24	16.23	19.66	22.52	23.63	22.21	19.39	15.62	11.87
Maximum Temperature, C°	21.03	23.09	26.31	30.62	32.95	33.48	33.56	33.30	32.90	31.33	27.25	23.21
Average Temperature, C°	14.95	14.88	16.23	18.84	22.03	25.11	26.86	27.44	26.21	23.81	20.38	16.91
RH (%)	68.96	68.47	68.01	65.57	65.37	66.29	67.91	68.01	66.36	66.58	66.90	68.08
U_2 (m/s)	4.39	4.39	4.34	4.19	4.03	4.15	4.30	4.06	3.91	3.78	3.89	4.12
Precipitation (mm/month)	29.45	20.19	10.68	6.06	0.39	0.26	0.00	0.00	0.13	5.32	16.13	25.91

Table (2)The average air temperature and annual precipitation values across the four decades within the study region.

Period	Temperature (°C)			Annual Precipitation (mm)
	Maximum	Minimum	Average	
1981-1990	34.2	9.2	20.8	111.27
1991-2000	34.8	9.7	20.9	98.61
2001-2010	35.2	10.0	21.3	93.34
2011-2021	35.8	10.0	21.6	151.14

2.2. Geology and soil unit

The geological composition of the area under study consisted primarily of Holocene Lacustrine sedimentary rocks with sabkha formations in the majority of regions, as well as Holocene Fluvial sedimentary rocks (Figure 2). As per the Key to Soil Taxonomy (Gad and Ali, 2011), the research area exhibits four distinct taxonomic soil units. In the northeast, there are common haploid organisms, whereas in the northeast and south-central regions, there are characteristic torripassament organisms. The eastern part of the territory is home to Vertic Torrifluvents, while Typic Torrifluvents occupy the remainder of the region. In conjunction with a raster methodology that simplifies calculations, ArcGIS Pro 2.7 is a mapping software that supports both raster and vector data (ESRI, 2021). Subsequently, the soil's potential uses were assessed and a more comprehensive understanding of its complexity and variability was achieved by superimposing classified EC, CaCO3, and depth maps onto the land.

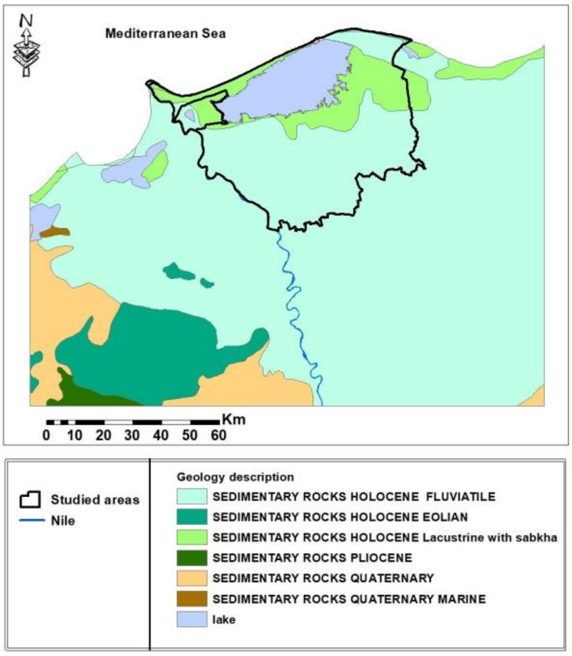

Figure (2). The geology of the study area.

2.3. Data sets

This study employed several datasets, specifically Landsat satellite images from the years 1972, 1984, 1998, 2002, 2010, 2015, and 2022. A total of 80 soil measurements, spanning an area of 156390.30 hectares. These observations were obtained from Earth Explorer on the US Geological Survey (https://earthexplorer.usgs.gov). Radar technology enabled the acquisition of the SRTM-DEM, enabling the precise mapping of the Earth's surface with an accuracy of one arc-second and intervals of 30 meters. The last update occurred in 2022 (**Bakr and Bahnassy, 2019**). The downloaded SRTM-DEM has been georeferenced and prepared for use in the ArcMap software. The methodology flowchart is shown in Figure (3).

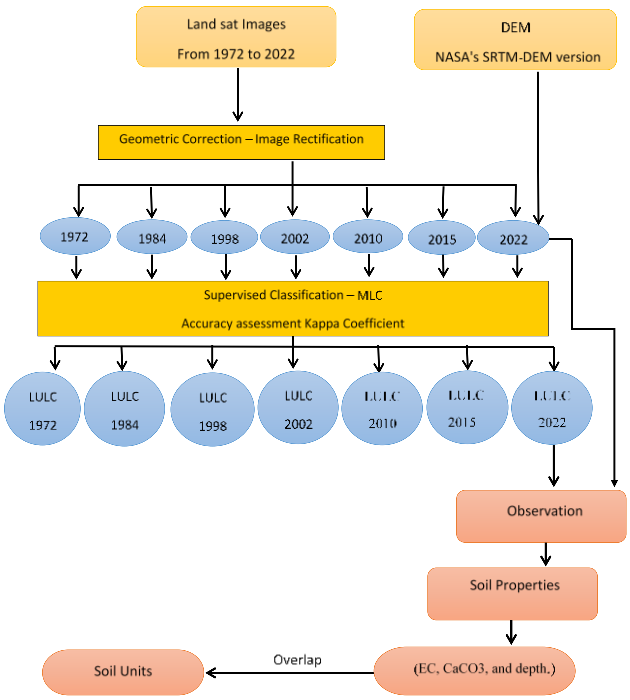

Figure (3). The methodology flowchart for the current research.

2.4. Satellite images preprocessing

The LULC analysis utilized seven Landsat satellite pictures spanning from 1972 to 2022, including data from the years 1972, 1984, 1998, 2002, 2010, 2015, and 2022. Table (3 presents data regarding the satellite pictures that were utilized. Furthermore, Table (4) presents a detailed depiction of the LULC classes. The satellite images were adjusted for geometric accuracy using scanned topographic maps and 80 ground truth points (GTPs) collected from the research region in 2022. The images were then aligned to Zone 36 and projected using the Universal Transverse Mercator (UTM) coordinate system with the World Geodetic System 1984 (WGS84) datum. The resulting image has an average root mean square error (RMSE) of 0.3 pixels. Since the images were acquired in July without any cloud cover, there was no need for atmospheric correction. For the study, the Landsat images were cropped to match the borders of the study area based on the 2022 image. The appropriate combination of bands was selected to improve visualization and accurately identify different Land Use and Land Cover (LULC) classes. ENVI 5.3 software was used for image preprocessing. *The Landsat images allocated for the study were subset to match the borders of the study area based on the 2022 image. The appropriate band combination was selected to enhance visualization, allowing for the differentiation of various training locations for different Land Use and Land Cover (LULC) classes with improved accuracy. Image preprocessing was conducted using ENVI 5.3 Software (ENVI, 2015).*

Table (3). The present study used Landsat *satellite images.*

Year	LANDSAT Satellite	Scene ID	Path/Row	Pixel Size	Sun Elevation	Sensor ID*	No. of Bands
1972	LS-1	LM11910381972263AAA04	191/038	60	50.37	MSS	4
1984	LS-5	LT51770381984255XXX04	177/038	30	51.72	TM	7
1998	LS-5	LT51770381998245RSA03	177/038	30	55.33	TM	7
2002	LS-5	LT51770382002101XXX01	177/038	30	55.09	TM	7
2010	LS-5	LT51770392010198MTI00	177/039	30	64.92	TM	7
2015	LS-8	LC81770392015116LGN00	177/039	30	63.78	OLI_TIRS	11
2022	LS-8	LC91770382022207LGN00	177/038	30	68.72	OLI_TIRS	11

MSS: Multispectral Scanner; TM: Thematic Mapper; OLI: Operational Land Imager; TIRS: Thermal Infrared Sensor.

Table (4). Key land use and land cover categories in the research region

LULC Classes	Description
Bare soils	Includes uncultivated lands, dunes, and built-up land (residential, commercial, roads, …etc)
Agricultural land	Cultivated land with all types of crops
Fish farms	Established around Burullus Lake
Water bodies	Mainly Burullus Lake
Natural vegetation	The natural plants that cover the surface of the study area

2.5. Land use/land cover classification

The research region was classified into five distinct LULC groups: bare soils, agricultural land, fish farms, water bodies, and natural vegetation. Then these classifications are through the visual interpretation of satellite images and field excursions. We identified specific training sites for each LULC class using the Maximum Likelihood Classifier (MLC) method. Using these training samples, we generated a signature file containing the multivariate statistics for each LULC class. We then applied the MLC algorithm using this signature file as input. Despite its simplified configurations, the MLC method maintained satisfactory performance, achieving high accuracy levels. Moreover, it demonstrated improved performance even with a reduced number of training samples **(Li et al., 2014; Valero Medina and Alzate Atehortúa, 2019)**. While contemporary machine learning algorithms (MLA) like support vector machines (SVM), artificial neural networks (ANN), and random forests (RF) are often recognized for their higher accuracy, the assertion that the maximum likelihood classifier (MLC) maintains validity persists.

2.6. The evaluation of the accuracy of classified images

The reliability of the spatial information derived from remote sensing images for accurate image classification is determined by accuracy evaluation processes (Ibharim et al. 2015; Lin et al. 2015). When integrated with ground control points that function as a reference, remotely sensed spatial information is both precise and dependable (Congalton and Green 2019). Consequently, the accuracy of each categorized image was assessed and determined by calculating the producer's accuracy, user's accuracy, overall accuracy, and Kappa coefficient values (Zhang et al. 2016). Furthermore, the Markov model, GIS, and RS data were successfully integrated as a result of the nature of GIS and its incorporation with remote sensing (RS). Consequently, thematic maps of various LULC for the investigated periods were generated using ArcGIS 10.8 software. This assessment covered images from 1972, 1984, 1998, 2002, 2010, 2015, and 2022, aiming to determine overall accuracy and conduct kappa analysis. We applied 50 ground truth points (GTPs) and performed visual interpretation using Google Earth to verify the accuracy. Then computed the overall accuracy and kappa coefficient for the two datasets using the equations provided **(Vivekananda et al., 2021).**

$$\text{Overall Accuracy(OA)} = \frac{1}{N}\sum_{k=1}^{r} n_i$$

$$\text{Kappa coefficient(k)} = \frac{N\sum_{k=1}^{r}\chi_{kk} - \sum_{k=1}^{r}\left(\chi_{k+}\cdot\chi_{+k}\right)}{N^2 - \sum_{k=1}^{r}\left(\chi_{k+}\cdot\chi_{+k}\right)}$$

Where: N represents the total number of pixels, r represents the number of classes, χ_{kk} represents the total pixels in row "k" and column "k," χ_{k+} represents the total samples in row "k," and represents the total samples in column "k" in the error matrix.

3. RESULTS AND DISCUSSION

3.1. Digital Elevation Model (DEM)

The findings reveal that land surface elevation within the study area ranged from -1 to 7 meters in 2022. To delineate the extent of each elevation category, the Digital Elevation Model (DEM) underwent classification, as depicted in Figure (4). The analysis uncovered significant variability in land surface elevation in 2022, with roughly 10.05% of the landmass lying within an altitude range of 0 to 7 meters above sea level (ASL). However, the most prominent area was situated at the minimum altitude (<0, BSL). In 2022, elevations below zero encompassed approximately 89.95% of the study area, as illustrated in Figure 5.

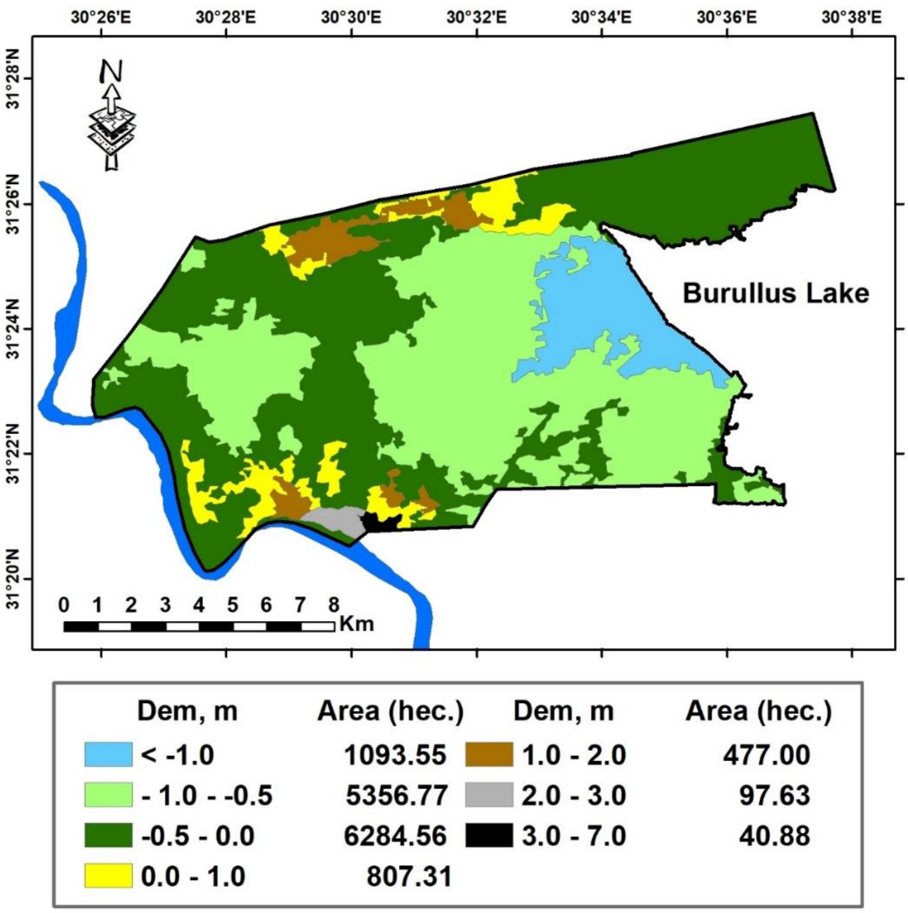

Figure (4). The DEM (Digital Elevation Model) image of the research area in 2022

3.2. Land Use/Land Cover Change (LULCC)

The Maximum Likelihood classifier (MLC) was used as a supervised classification technique to produce the final Land Use and Land Cover (LULC) classified thematic maps for the years 1972, 1984, 1998, 2013, and 2022 (Figure 5). In addition, Table (5) and (Figure 6) display the total area in hectares and the percentage of various land use and land cover (LULC) classes in the study area for the given dates.

Table (5). The percentage of the total area covered by each LULC class in the classified maps of the study region between the years 1972 and 2022, expressed as hectares (ha) and percentages (%)

Year	unit	Land use/land cover classes					
		Water bodies	Natural vegetation	Fish farms	Agricultural Land	Bare soil	Total
1972	Ha	21055.12	7492.43	0.00	88543.27	39759.06	156849.87
	%	13.42	4.78	0.00	56.45	25.35	
1984	Ha	16507.26	8747.66	0.00	88847.73	42518.24	156620.88
	%	10.52	5.58	0.00	56.65	27.11	
1998	ha	12701.97	7271.67	7580.39	98625.18	30229.19	156408.40
	%	8.10	4.64	4.83	62.88	19.27	
2002	ha	10453.93	8886.44	13780.49	102668.04	20601.37	156390.26
	%	6.66	5.67	8.79	65.46	13.13	
2010	ha	11090.18	7123.75	14713.68	95871.61	27591.02	156390.25
	%	7.07	4.54	9.38	61.12	17.59	
2015	ha	10219.41	8406.70	14451.58	97039.68	26272.89	156390.26
	%	6.52	5.36	9.21	61.87	16.75	
2022	ha	9981.56	9213.06	13375.62	99387.49	24432.52	156390.26
	%	6.36	5.87	8.53	63.36	15.58	
Change, ha/year	ha	-221.47	34.41	241.47	216.88	-306.53	

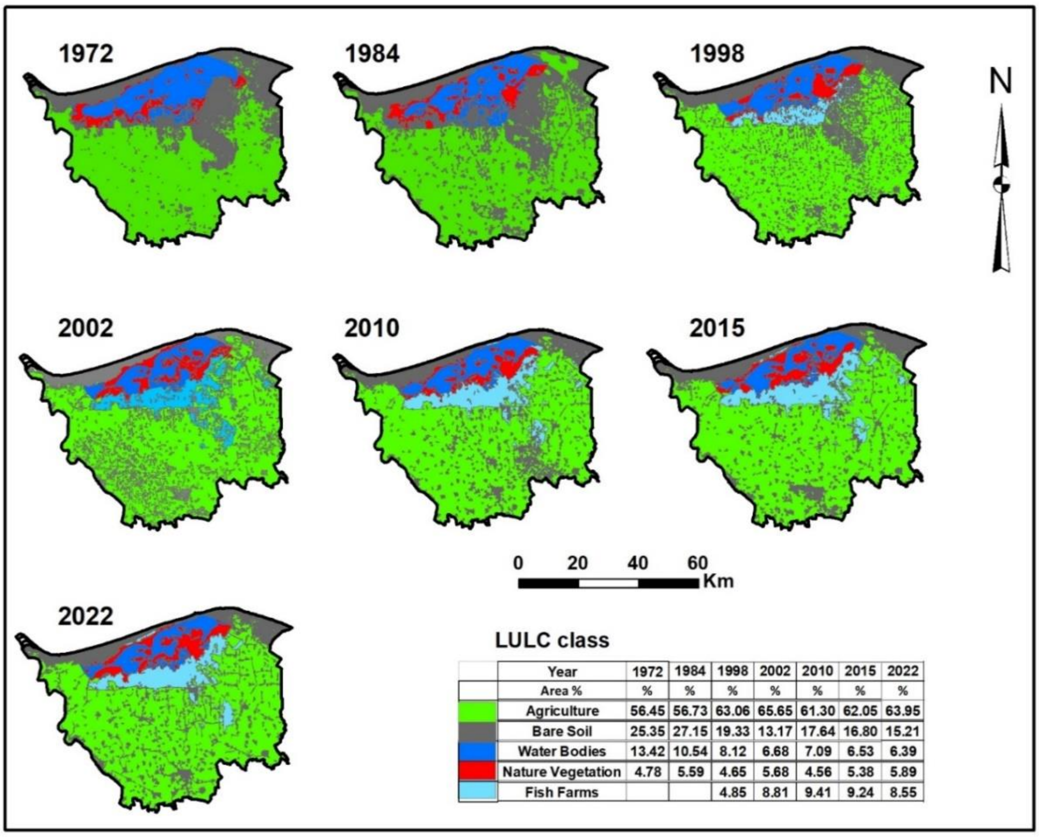

Figure (5). Maps illustrating the classification of different land use/land cover classes in the study area from 1972 to 2022 were generated.

The findings (Figure 5 and Table 5) demonstrate the presence of five primary land use and land cover (LULC) categories in the study area: barren soils, cultivated land, aquaculture facilities, indigenous vegetation, and bodies of water. Our findings reveal that fish farms, initially established in the study area in 1998, have rapidly expanded, taking up approximately 9.21% and 8.55% of the designated research area in 2015 and 2022, respectively. In contrast, water bodies have decreased significantly over time. In 2022, this group accounted for around 6.36% of the study area, a decline from 13.42% in 1972. The findings of the LULC transformation are consistent with the observations in the Kafr El-Shiekh governorate, Egypt, which exhibited a comparable state **(Bakr and Afifi, 2019).** It was determined that fish farms had not been observed before and had recently started to develop around Burullus Lake approximately in 1998. From 1972 to 2022, the proportion of bare soil decreased, dropping from 25.35% in 1972 to 15.58% in 2022. In 1998, there was a 6.08% decrease in the extent of exposed soil, indicating that efforts to restore the land may have focused on the sand sheet located in the northeastern portion of the research area.

The study area is predominantly characterized by agricultural land, which occupies a vast expanse. It experienced significant growth over time due to government reclamation initiatives. Specifically, between 1972 and 2022, it increased from 56.45% to 63.36%, respectively. We computed the mean overall pattern for the land use and land cover (LULC) categories. The water bodies experienced a decrease of 221.47 hectares per year over 50 years. Furthermore, the cultivation activity reduced the bare soil by 306.53 hectares per year. The area of natural vegetation, fish farms, and agricultural soil increased by 34.41, 241.47, and 216.88 hectares per year, respectively, over 50 years. **(Abd El-Hamid et al., 2021)** suggest that the terrestrial areas surrounding the Egyptian deltaic lakes (Manzala, Burullus, Idku, and Mariout) may experience similar levels of environmental and human-induced pressures over 80 years. Primary stressors on these ecosystems include the establishment of fish farms and the expansion of cultivated land on barren soils.

3.3. **Assessment of accuracy**

For each classified map in Figure (5), we derived the kappa coefficient and overall accuracy from satellite images taken in 1972, 1984, 1998, 2002, 2010, 2015, and 2022. Table 6 displays the final values for these parameters. According to **(Lea and Curtis, 2010),** the overall accuracy of all classified photos is deemed satisfactory. Their percentages ranged from 88% to 96%. Moreover, Table (6) demonstrates that the kappa coefficients ranged from 0.86 to 0.95. This indicates that there is a substantial level of concurrence between the produced and authentic classified maps.

Table (6). shows the overall accuracy and kappa coefficient for the maximum likelihood classification of images in 1972, 1984, 1998, 2002, 2010, 2015, and 2022.

Year	1972	1984	1998	2002	2010	2015	2022
Overall Accuracy	0.900	0.960	0.900	0.883	0.917	0.900	0.950
Kappa coefficient	0.875	0.950	0.880	0.860	0.900	0.880	0.940

The results indicate that the MLC has the potential to provide a reliable and precise assessment of land use and land cover change in the study area. The findings are consistent with the studies conducted by **(Bakr and Abd El-kawy, 2020).** The study's findings also showed that using geo-informatics, remote sensing, GIS, and modeling is effective for making changes to land use and land cover (LULC) and mapping, monitoring, and managing resources.

The changes in land use and cover related to agriculture in river basin regions have a significant impact on the development of nations that depend on agriculture as a major part of their economy. Emphasizing agricultural activities in domestic policies has significant implications, particularly for the lower regions of these river basins. This study emphasizes the significance of promptly evaluating sustainability indicators for land and water resources in the entire Nile Delta, especially in the coastal zone. It is crucial to have information on LULC change and the factors influencing these changes for effective long-term planning, as they provide additional insights. Long-term data can uncover positive findings about LULC change and its effects. It is crucial to consistently track this data in conjunction with the research progress. Future research should concentrate on analyzing the changes in land use and land cover within the basin using multi-criteria evaluations. This will offer an additional understanding of how population growth and climate change impact the water, vegetation, and wildlife in river basins. The results of this research would be useful in determining effective methods for improving the Nile Delta and identifying upcoming dangers that require immediate action to protect the longevity of the basin's resources.

3.4. Soil units

Based on the soil unit map (Figure 6) approximately 12% of the research area's northern shoreline along the Mediterranean consists of saline soils. Non-saline soils comprise 10% of the research area. The remaining portion of the research region consists of moderately salinized soils. The findings are consistent with **(Alfiky et al., 2012)** research stated that the study area's northern section is classified as "River Shelf Lands" while the southern part is categorized as "Marine River Sedimentary Lands." The Lake area consists of three distinct components: Burullus Lake, fish farms, and natural vegetation that encompasses a portion of the study area (Figure 6).

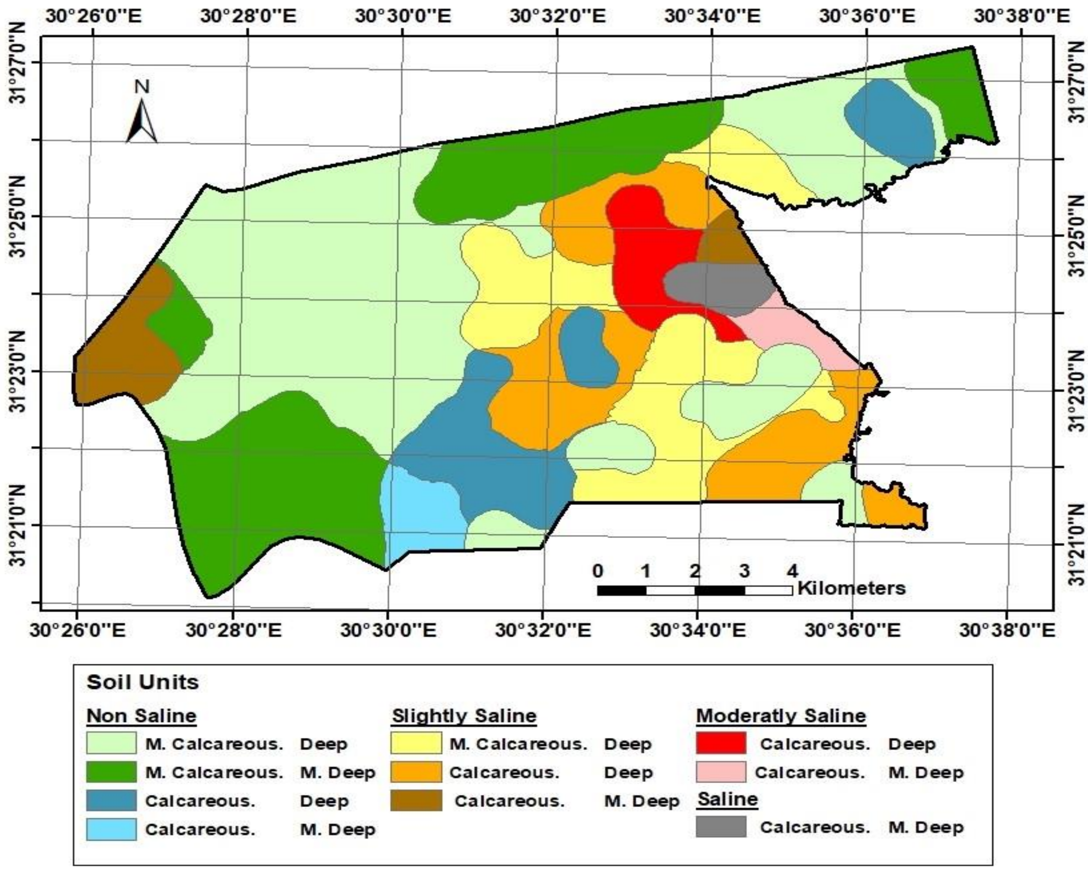

Figure (6). Soil units of the studied area.

Conclusion

The study demonstrated the effectiveness of using remote sensing and GIS techniques to analyze LULC changes in the Motobus region of the Nile Delta in Egypt between 1972 and 2022. The supervised maximum likelihood classification of Landsat satellite images reliably identified and mapped five LULC classes - bare soil, agricultural land, fish farms, natural vegetation, and water bodies. Accuracy assessment confirmed the high classification accuracy. Over the past 50 years, agricultural land has increased considerably, from 56.46% to 63.36% of the total area, largely attributed to land reclamation efforts. In contrast, water bodies and bare soils showed significant declines, with water bodies falling from 13.42% to 6.36%. Fish farms emerged in 1998 and expanded rapidly to cover 8.53% by 2022. The digital elevation model analysis highlighted that around 90% of the study area lies below sea level, indicating high vulnerability to flooding from sea level rise. The LULC change detection results can guide regional land use planning policies and practices. The study emphasizes the value of regularly monitoring LULC modifications using earth observation data to support informed decision-making for sustainable land management.

REFERENCES

Abd El-Hamid, H.T., El-Alfy, M.A., & Elnaggar, A.A. (2021). Prediction of future situation of land use/cover change and modeling sensitivity to pollution in Edku Lake, Egypt based on geospatial analyses. *GeoJournal, 86*, 1895-1913

Adepoju, M., Millington, A., & Tansey, K. (2006). Land use/land cover change detection in metropolitan Lagos (Nigeria): 1984–2002. In, *ASPRS 2006 Annual Conference Reno, Nevada May* (pp. 1-5)

Alfiky, A., Kaule, G., & Salheen, M. (2012). Agricultural fragmentation of the Nile Delta; a modeling approach to measuring agricultural land deterioration in Egyptian Nile Delta. *Procedia Environmental Sciences, 14*, 79-97

Armin, M., Majidian, M., & Kheybari, V.G. (2020). Land use/land cover change detection and prediction in the Yasouj City suburbs in Kohgiluyeh Va Boyerahmad Province in Iran. *Arid Ecosystems, 10*, 203-210

Arowolo, A.O., & Deng, X. (2018). Land use/land cover change and statistical modelling of cultivated land change drivers in Nigeria. *Regional environmental change, 18*, 247-259

Bakr, N., & Abd El-kawy, O.R. (2020). Modeling the artificial lake-surface area change in arid agro-ecosystem: A case study in the newly reclaimed area, Egypt. *Journal of Environmental management, 271*, 110950

Bakr, N., & Afifi, A.A. (2019). Quantifying land use/land cover change and its potential impact on rice production in the Northern Nile Delta, Egypt. *Remote Sensing Applications: Society and Environment, 13*, 348-360

Bakr, N., & Bahnassy, M.H. (2019). Egyptian natural resources. *The Soils of Egypt*, 33-49

Calicioglu, O., Flammini, A., Bracco, S., Bellù, L., & Sims, R. (2019). The future challenges of food and agriculture: An integrated analysis of trends and solutions. *Sustainability*, *11*, 222

Chi, G., & Ho, H.C. (2018). Population stress: A spatiotemporal analysis of population change and land development at the county level in the contiguous United States, 2001–2011. *Land use policy*, *70*, 128-137

Cihlar, J. (2000). Land cover mapping of large areas from satellites: status and research priorities. *International journal of remote sensing, 21*, 1093-1114

Congalton, R.G., & Green, K. (2019). *Assessing the accuracy of remotely sensed data: principles and practices*. CRC press

Das, S., & Sarkar, R. (2019). Predicting the land use and land cover change using Markov model: A catchment level analysis of the Bhagirathi-Hugli River. *Spatial Information Research, 27*, 439-452

Derdouri, A., Wang, R., Murayama, Y., & Osaragi, T. (2021). Understanding the links between LULC changes and SUHI in cities: Insights from two-decadal studies (2001–2020). *Remote Sensing*, *13*, 3654

Dewan, A.M., & Yamaguchi, Y. (2009). Using remote sensing and GIS to detect and monitor land use and land cover change in Dhaka Metropolitan of Bangladesh during 1960–2005. *Environmental monitoring and assessment, 150,* 237-249

El-Shihy, A.A., & Ezquiaga, J.M. (2019). Architectural design concept and guidelines for floating structures for tackling sea level rise impacts on Abu-Qir. *Alexandria Engineering Journal, 58,* 507-518

El Kafrawy, S.B., Bek, M., & Negm, A.M. (2019). An overview of the Egyptian northern coastal lakes. *Egyptian Coastal Lakes and Wetlands: Part I: Characteristics and Hydrodynamics*, 3-17

Field, C.B., Barros, V.R., Mach, K.J., Mastrandrea, M.D., van Aalst, R., Adger, W.N., Arent, D.J., Barnett, J., Betts, R.A., & Bilir, T.E. (2014). Technical summary

Gad, A.-A., & Ali, R. (2011). Creation of GIS digital land resources database of the Nile delta, Egypt, for optimal soil management. *Procedia-Social and Behavioral Sciences, 19*, 641-650

Gomes, L., Bianchi, F., Cardoso, I., Schulte, R., Arts, B., & Fernandes Filho, E.I. (2020). Land use and land cover scenarios: An interdisciplinary approach integrating local conditions and the global shared socioeconomic pathways. *Land use policy*, *97*, 104723

Halim, A.M.A., Mahmoud, M.G., Guerguess, M.S., & Tadros, H.R. (2013). Major constituents in Lake Edku water, Egypt. *The Egyptian Journal of Aquatic Research, 39*, 13-20

Hou, H., Wang, R., & Murayama, Y. (2019). Scenario-based modelling for urban sustainability focusing on changes in cropland under rapid urbanization: A case study of Hangzhou from 1990 to 2035. *Science of the total environment, 661*, 422-431

Hua, A.K. (2017). Land use land cover changes in detection of water quality: a study based on remote sensing and multivariate statistics. *Journal of environmental and public health, 2017*

Ibharim, N., Mustapha, M., Lihan, T., & Mazlan, A. (2015). Mapping mangrove changes in the Matang Mangrove Forest using multi temporal satellite imageries. *Ocean & coastal management*, *114*, 64-76

Iizuka, K., Johnson, B.A., Onishi, A., Magcale-Macandog, D.B., Endo, I., & Bragais, M. (2017). Modeling future urban sprawl and landscape change in the Laguna de Bay Area, Philippines. *Land*, *6*, 26

Jawak, S.D., Devliyal, P., & Luis, A.J. (2015). A comprehensive review on pixel oriented and object oriented methods for information extraction from remotely sensed satellite images with a special emphasis on cryospheric applications. *Advances in Remote Sensing, 4*, 177-195

Kotaridis, I., & Lazaridou, M. (2018). Environmental change detection study in the wider area of lignite mines. *Civil Engineering and Architecture*, *6*, 108-114

Lea, C., & Curtis, A. (2010). Thematic accuracy assessment procedures: National Park Service vegetation inventory, version 2.0. *Natural resource report NPS/2010/NRR—2010/204. National Park Service, Fort Collins, Colorado*

Li, C., Wang, J., Wang, L., Hu, L., & Gong, P. (2014). Comparison of classification algorithms and training sample sizes in urban land classification with Landsat thematic mapper imagery. *Remote Sensing*, *6*, 964-983

Lin, C., Wu, C.-C., Tsogt, K., Ouyang, Y.-C., & Chang, C.-I. (2015). Effects of atmospheric correction and pansharpening on LULC classification accuracy using WorldView-2 imagery. *Information Processing in Agriculture, 2*, 25-36

Liping, C., Yujun, S., & Saeed, S. (2018). Monitoring and predicting land use and land cover changes using remote sensing and GIS techniques—A case study of a hilly area, Jiangle, China. *PloS one*, *13*, e0200493

Lombardi, J.V., Perotto-Baldivieso, H.L., & Tewes, M.E. (2020). Land cover trends in South Texas (1987–2050): potential implications for wild felids. *Remote Sensing, 12*, 659

Masria, A., Negm, A., Iskander, M., & Saavedra, O. (2014). Coastal zone issues: a case study (Egypt). *Procedia Engineering, 70,* 1102-1111

Nath, B., Wang, Z., Ge, Y., Islam, K., P. Singh, R., & Niu, Z. (2020). Land use and land cover change modeling and future potential landscape risk assessment using Markov-CA model and analytical hierarchy process. *ISPRS International Journal of Geo-Information*, *9*, 134

Nofal, E., Amer, M., El-Didy, S., & Fekry, A.M. (2015). Delineation and modeling of seawater intrusion into the Nile Delta Aquifer: a new perspective. *Water Science*, *29*, 156-166

Phiri, D., & Morgenroth, J. (2017). Developments in Landsat land cover classification methods: A review. *Remote Sensing, 9*, 967

Radwan, T.M. (2019). Monitoring agricultural expansion in a newly reclaimed area in the western nile delta of Egypt using landsat imageries. *Agriculture, 9*, 137

Rawat, J., & Kumar, M. (2015). Monitoring land use/cover change using remote sensing and GIS techniques: A case study of Hawalbagh block, district Almora, Uttarakhand, India. *The Egyptian Journal of Remote Sensing and Space Science, 18*, 77-84

Reimann, L., Vafeidis, A.T., Brown, S., Hinkel, J., & Tol, R.S. (2018). Mediterranean UNESCO World Heritage at risk from coastal flooding and erosion due to sea-level rise. *Nature communications, 9*, 4161

Saadat, H., Adamowski, J., Bonnell, R., Sharifi, F., Namdar, M., & Ale-Ebrahim, S. (2011). Land use and land cover classification over a large area in Iran based on single date analysis of satellite imagery. *ISPRS Journal of Photogrammetry and Remote Sensing, 66*, 608-619

Srivastava, P.K., Han, D., Rico-Ramirez, M.A., Bray, M., & Islam, T. (2012). Selection of classification techniques for land use/land cover change investigation. *Advances in Space Research*, *50*, 1250-1265

Valero Medina, J.A., & Alzate Atehortúa, B.E. (2019). Comparison of maximum likelihood, support vector machines, and random forest techniques in satellite images classification. *Tecnura, 23*, 13-26

Vivekananda, G., Swathi, R., & Sujith, A. (2021). Multi-temporal image analysis for LULC classification and change detection. *European journal of remote sensing, 54*, 189-199

Yan, W.Y., Shaker, A., & El-Ashmawy, N. (2015). Urban land cover classification using airborne LiDAR data: A review. *Remote sensing of Environment*, *158*, 295-310

Yuan, F., Sawaya, K.E., Loeffelholz, B.C., & Bauer, M.E. (2005). Land cover classification and change analysis of the Twin Cities (Minnesota) Metropolitan Area by multitemporal Landsat remote sensing. *Remote sensing of Environment, 98*, 317-328

Zabihi, M., Moradi, H., Gholamalifard, M., Khaledi Darvishan, A., & Fürst, C. (2020). Landscape management through change processes monitoring in Iran. *Sustainability, 12*, 1753

Zhang, Z., Liu, S., Wei, J., Xu, J., Guo, W., Bao, W., & Jiang, Z. (2016). Mass change of glaciers in Muztag Ata–Kongur Tagh, Eastern Pamir, China from 1971/76 to 2013/14 as derived from remote sensing data. *PloS one, 11*, e0147327

الملخص العربي

استخدام الصور الفضائية لتحليل تغييرات استخدام الأراضي وتغطية الأراضي (LULC) في النظام البيئي لمنطقة مطوبس، دلتا النيل، مصر

عزه عزت عبد الوكيل الشرقاوى[1] ايهاب محرم محمد مرسي[2] جمال عبد الناصر خليل[1]

وفاء حسن محمد علي[1] هدى عبد الفتاح محمود[1]

1 كلية الزراعة سابا باشا – جامعة الاسكندرية – مصر

2 معهد بحوث الاراضي والمياه والبيئة – مركز البحوث الزراعية – الجيزة – مصر

إن فهم الديناميكيات المتغيرة لاستخدام الأراضي والغطاء الأرضي (LULC) أمر بالغ الأهمية لتعديل الإدارة البيئية الفعالة والتخطيط المستدام لاستخدام الأراضي. يهدف هذا العمل إلى تحديد وتصنيف سبع صور التقطتها الأقمار الصناعية لاندسات على مدى 50 عامًا في النظام البيئي لمنطقة دلتا النيل في مصر. في هذه الدراسة، تم إجراء الكشف عن ديناميكيات التغير الزمني لتغير الأراضي والتربة والحياة البرية في الفترة من عام 1972 إلى عام 2022. استخدمنا سبع صور لاندسات، تم الحصول عليها بواسطة أجهزة استشعار مختلفة، كمصادر للبيانات المكانية والزمانية لمنطقة الدراسة. علاوة على ذلك، استخدمت عملية تصنيف الصور بطريقة تصنيف خاضعة للإشراف. أظهرت نتائج تقدير التغير في التربة والتغير في الأراضي والمياه بين عامي 1972 و2022 أن نسبة المناطق المبنية في منطقة الدراسة ارتفعت من 5.5% في عام 1972 إلى 12.5% في عام 2022. وقد جاء هذا التوسع العمراني على حساب تحويل الأراضي الزراعية السابقة إلى مدن وقرى قائمة، وكذلك بناء مناطق سكنية جديدة على أراضٍ غير مبنية. بالإضافة إلى ذلك، ارتفعت نسبة الأراضي المزروعة من 56.45% من المساحة الإجمالية في عام 1972 إلى 63.55% في عام 2022، ويرجع ذلك أساسًا إلى مبادرات استصلاح الاراضي المستمرة في المناطق الصحراوية خارج وادي النيل. علاوة على ذلك، شهدت المناطق الصحراوية في الفترة من 1972 إلى 2022 انخفاضًا كبيرًا في إجمالي مساحة الأراضي الصحراوية حيث فقدت حوالي 50% من مساحتها الأصلية، بينما شهدت المسطحات المائية توسعًا ضئيلًا لا يكاد يذكر. تتسم هذه الاتجاهات بانخفاض في المناطق الصحراوية وزيادة في المناطق الحضرية والزراعية المستعادة مؤخرًا. فيما يتعلق بالتحقق من صحة نموذج CA-Markov، تراوحت مؤشرات Kappa بين 0.86 و0.93 لكل من الخرائط الفعلية والمحاكاة. وهذا يشير إلى أن النموذج كان أداؤه جيدًا بشكل استثنائي في التنبؤ بالاتجاهات المستقبلية في الأراضي والتربة والمياه والتغير المناخي. ولذلك، فإن استخدام النموذج الهجين CA-Markov للتنبؤ بالاتجاهات المستقبلية لتغير الأراضي وتغيير استخدام الأراضي والحراجة ونمذجتها هو وسيلة واعدة لرصد الآثار السلبية لتغيرات استخدام الأراضي وتغيير التربة والتغير في الأراضي والتغير في استخدام الأراضي والتخفيف من حدتها. كما يساعد هذا النهج صانعي سياسات استخدام الأراضي ويسهل إدارة الأراضي.